Effect of Surface Nanotopography on Bone Response to Titanium Implant

Gileade P. Freitas, DDS, MSc[1]
Helena B. Lopes, DDS, MSc[1]
Evandro C. Martins-Neto, DDS, MSc[1]
Paulo T. de Oliveira, DDS, MSc, PhD[2]
Marcio M. Beloti, DDS, MSc, PhD[2]
Adalberto L. Rosa, DDS, MSc, PhD[2]*

Clinical success of implant therapy is directly related to titanium (Ti) surface properties and the quality of bone tissue. The treatment of Ti implants with H_2SO_4/H_2O_2 is a feasible, reproducible, and low-cost technique to create surface nanotopography (Ti-Nano). As this nanotopography induces osteoblast differentiation, we hypothesized that it may affect bone response to Ti. Thus, this study was designed to evaluate the bone response to a machined Ti implant treated with H_2SO_4/H_2O_2 to generate Ti-Nano and to compare it with a commercially available microtopographic Ti implant (Ti-Porous). Implants were placed in rabbit tibias and evaluated after 2 and 6 weeks, and the bone tissue formed around them was assessed by microtomography to record bone volume, bone surface, specific bone surface, trabecular number, trabecular thickness, and trabecular separation. Undecalcified histological sections were used to determine the percentages of bone-to-implant contact, bone area formed between threads, and bone area formed in the mirror area. At the end of 6 weeks, the removal torque was evaluated using a digital torque gauge. The results showed bone formation in close contact with both Ti-Nano and Ti-Porous implants without relevant morphological and morphometric differences, in addition to a similar removal torque irrespective of surface topography. In conclusion, our results have shown that a simple and low-cost method using H_2SO_4/H_2O_2 is highly efficient for creating nanotopography on Ti surfaces, which elicits a similar bone response compared with microtopography presented in a commercially available Ti implant.

Key Words: biocompatibility, bone, dental implant, nanomodified surface, titanium

INTRODUCTION

One of the focuses of the implantology field is the development of titanium (Ti) surfaces to elicit enhanced and high-quality osseointegration, mainly in challenging bone sites. Among the treatments, some acids, such as HCl, H_2SO_4, and H_3PO_4, are widely used to modify Ti surface topography at the micro and nanoscale levels.[1–4] It has been shown that Ti with microtopography modulates osteoblast cell response and enhances contact osteogenesis.[5–7] Recently, several studies have highlighted that nanotopography regulates osteoblast activity and ultimately may affect bone response to Ti.[8–12]

The treatment with a mixture of H_2SO_4/H_2O_2 creates a physically and chemically well-characterized nanotopography on the Ti surface.[13,14] This nanotopography presents nanopits with an average size of 22 nm, which generates a 3-fold increase in the surface roughness, a thicker TiO_2 layer, and low rates of contaminants such as N and Si compared with an untreated Ti surface.[13] Regarding the commercial development of surface modifications, the treatment with H_2SO_4/H_2O_2 represents a very feasible, reproducible, and low-cost technique to generate nanotopography on Ti implants. Previous results of our group showed the osteogenic potential of this Ti with nanotopography in cells derived from distinct species and sites, such as human and rat bone marrow, and rat calvarial.[1,10,11,15] In addition, we determined mechanisms involving an $\alpha1\beta1$ integrin signaling pathway and a miR-SMAD-BMP2 circuit in the osteoinductive effect of Ti with nanotopography.[10,11]

Considering the promising in vitro results, it is of relevance to investigate the in vivo response of bone tissue to this nanotopography produced by H_2SO_4/H_2O_2 surface treatment. Thus, our aim was to evaluate the bone response to a machined Ti implant treated with a mixture of H_2SO_4/H_2O_2 to generate nanotopography and to compare it with a commercially available microtopographic Ti implant by placing them in rabbit tibias.

MATERIALS AND METHODS

Preparation of Ti implants

In this study, 36 self-tapping screw-type Ti implants (3.75 × 8.5 mm) with 2 different surfaces were used: (1) commercially

[1] Department of Oral and Maxillofacial Surgery and Periodontology, School of Dentistry of Ribeirão Preto, University of São Paulo, Ribeirão Preto, SP, Brazil.
[2] Department of Morphology, Physiology and Basic Pathology, School of Dentistry of Ribeirão Preto, University of São Paulo, Ribeirão Preto, SP, Brazil.
* *Corresponding author,* e-mail: adalrosa@forp.usp.br
DOI: 10.1563/aaid-joi-D-14-00254

available surface (Ti-Porous) produced by acid etching with a combination of NHO_3, HCL, and H_2SO_4 (Porous Conexão Sistemas de Prótese, Arujá, SP, Brazil) and (2) nanotopography surface (Ti-Nano). To generate the nanotopography, machined Ti implants (Conexão Sistemas de Prótese) were chemically treated with a solution consisting of equal volumes of H_2SO_4, 10 N, and H_2O_2 30% for 4 hours at room temperature under continuous agitation. All procedures were performed in a laminar flow cabinet to ensure sterile conditions of implants during the chemical etching. Some implants were examined by high-resolution, field emission scanning electron microscopy (SEM) using a microscope Inspect S50 (FEI Company, Hillsboro, Ore), operated at 25 kV.

Surgical procedures

For this study, 18 male New Zealand white rabbits (ranging from 3.5 to 4.5 kg) were used, and all procedures were performed according to the research protocols approved by the Ethics Committee in Animal Research of the School of Dentistry of Ribeirão Preto, University of São Paulo. Each rabbit received 2 implants randomly distributed in such way that 6 implants of each treatment were used for micro-computerized tomography (micro-CT) and histomorphometric analyses at 2 and 6 weeks, and for removal torque analysis at 6 weeks. The animals were anesthetized using a subcutaneous injection of acepromazine 1 mg/kg (União Química, Embuguaçú, SP, Brazil), followed by an intramuscular injection of xylazine 5 mg/kg (União Química) and ketamine hydrochloride 25 mg/kg (União Química). After skin preparation, mepivacaine 2% with epinephrine 1:100 000 (DFL, Rio de Janeiro, RJ, Brazil) was subcutaneously injected as local anesthetic. The medial region of the tibia was incised near to medial epiphysis to expose the area for implant placement. After site preparation using a sequence of drills, 1 implant was randomly placed in each tibia, and the wounds were closed with 4-0 nylon sutures (Shalon Fios Cirúrgicos, Goiânia, GO, Brazil). Postoperatively, all animals received analgesic (Tramal 0.02 mg/kg, Biolab Searle, São Paulo, SP, Brazil) and anti-inflammatory drugs (Profenid 3 mg/kg, Ketofen, Merial, São Paulo, SP, Brazil). After 2 and 6 weeks, the animals were euthanized, and the segments of tibias with the implants were processed for micro-CT and histomorphometric evaluations. The removal torque analysis was carried out only at 6 weeks.

Micro-CT analysis

After harvesting at 2 and 6 weeks, the bone segments were kept in 10% formalin buffered with 0.1 M sodium cacodylate, pH 7.3, for 48 hours and then transferred to a solution of 70% ethanol for 72 hours. Then, samples were submitted to micro-CT for morphometric analysis using the SkyScan 1172 system (Bruker-SkyScan, Kontich, Belgium). The images were acquired at 100 kVp, 100 mA, and 9.92 μm of resolution and reconstructed using the software NRecon (Bruker-Skyscan) with smoothing 4, ring artifact correction 12, and beam hardening correction 35%. The micro-CT analyses were carried out using the 3D Ctan software (Bruker-Skyscan) to measure bone volume, bone surface, specific bone surface, trabecular number, trabecular thickness, and trabecular separation. The region of interest in which these parameters were evaluated was established for each implant as a cylinder of 5.75-mm diameter and 7.0-mm high from the implant shoulder.

Histomorphometric analysis

After micro-CT analyses, bone segments were dehydrated, embedded in resin (LR White Hard Grade, London, UK), and sectioned using Exakt Cutting System (Exakt, Norderstedt, Germany). The longitudinal mesiodistal sections obtained were polished and mounted on acrylic slides using the Exakt Grinding System (Exakt). The resulting sections were stained with Stevenel's blue and Alizarin red. The histological description of tissues near to or in close contact with implants was based on light microscopy observations using a Leica DMLB light microscope (Leica, Bensheim, Germany). For each implant, measurements were taken from the first thread down toward the fourth both mesially and distally and used as the mean value of that implant. The amount of mineralized bone at the bone-implant interface was expressed as bone-to-implant contact (BIC) and between threads as bone area between threads (BABT). The amount of mineralized bone located outside the threads was determined as bone area within mirror area (BAMA). We previously defined this mirror area as a symmetric area to the trapezoid between 2 threads, sharing the larger base of the trapezoid.[16] The evaluations were performed using the ImageJ software, version 1.34 (National Institutes of Health, Bethesda, Md), by a single examiner who was calibrated and blinded to treatments.

Removal torque analysis

At 6 weeks, the sites were exposed and bone and soft tissues on the top of the implants were carefully removed. Subsequently, the force needed to unscrew the implants was measured using a digital torque gauge (Instruthem TQ680, São Paulo, SP, Brazil) and registered as the maximum removal torque.

Statistical analysis

The normality of data was determined using the Kolmogorov–Smirnov test. Then, the data of morphometric parameters and removal torque were obtained from 6 implants for each surface ($n = 6$) and submitted to either 2-way analysis of variance followed by Tukey test or Student *t* test. Differences at $P \leq .05$ were considered statistically significant.

Results

SEM analysis

Ti-Nano and Ti-Porous implant surfaces exhibited distinct topographical features. Ti-Nano implants at low magnification showed a smooth surface (Figure 1a), and high magnification revealed a surface characterized by a network of nanopores (Figure 1b). Ti-Porous implants at low magnification showed an irregular and homogeneous surface compared with Ti-Nano (Figure 1c), and implants at high magnification showed numerous cavities at the micrometer level (Figure 1d).

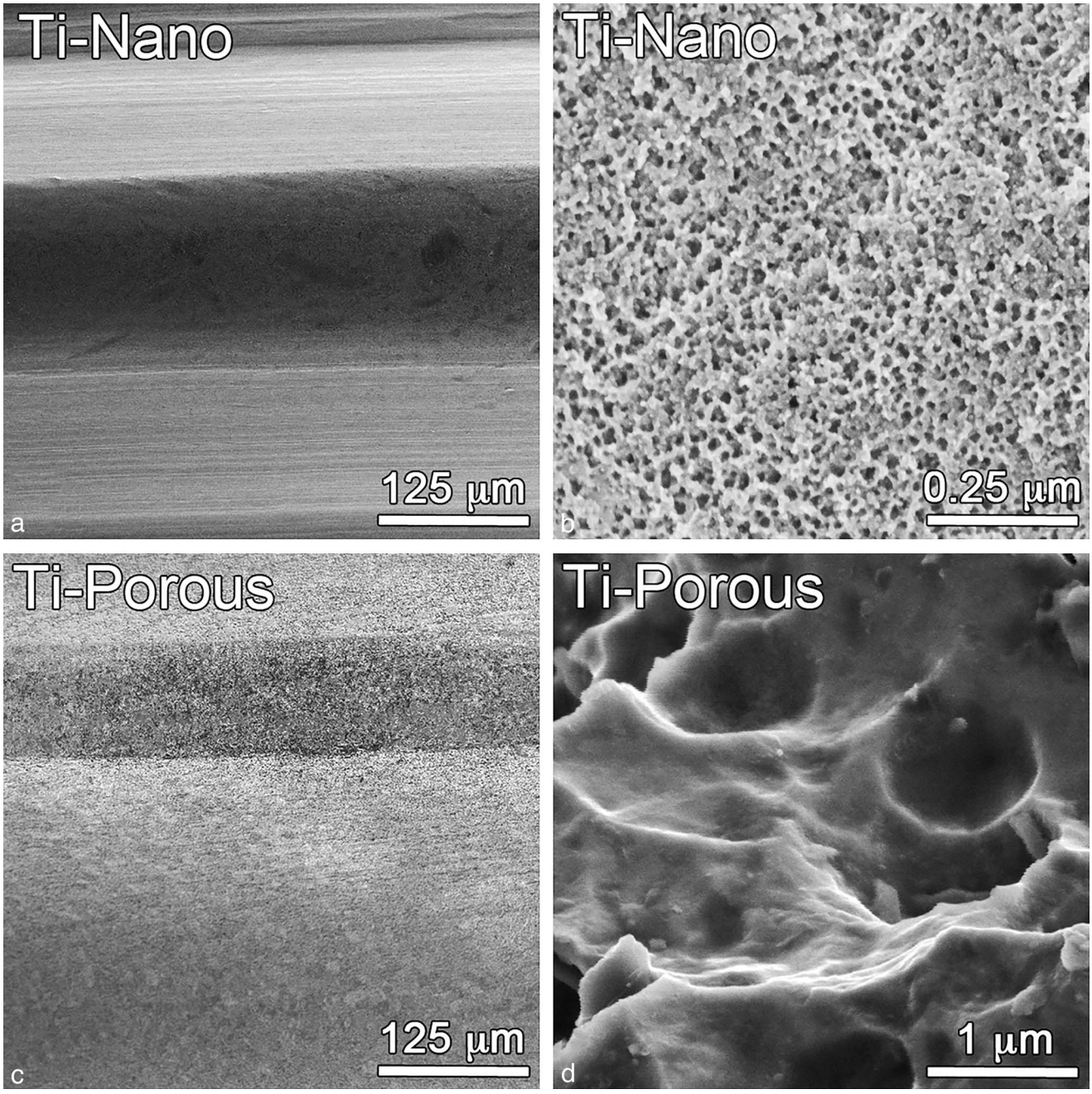

Figure 1. Field emission scanning electron microscopy images of Ti-Nano (a, b) and Ti-Porous (c, d) surfaces.

Micro-CT analysis

The 3-dimensional reconstructions obtained from micro-CT images showed an intimate contact between bone and implant surfaces in some areas without any meaningful difference related to surface topography of Ti implants or implantation time point (Figure 2a–d). It was observed that some bone trabeculae linked the implant surfaces to the cortical bone both at 2 and 6 weeks (Figure 2a–d). Bone volume was not affected by surface topography of Ti implants ($P = .842$), and it increased ($P = .035$) from 2 to 6 weeks (Figure 3a). Bone surface was not affected either by surface topography of Ti implants ($P = .505$) or by implantation time point ($P = .773$; Figure 3b). Specific bone surface was not affected by surface topography of Ti implants ($P = .510$), and it decreased ($P = .001$) from 2 to 6 weeks (Figure 3c). Trabecular number was not affected either by surface topography of Ti implants ($P = .407$) or by implantation time point ($P = .805$; Figure 3d). Trabecular thickness was not affected by surface topography of Ti implants ($P = .375$), and it increased ($P = .001$) from 2 to 6 weeks (Figure 3e). Trabecular separation was bigger on Ti-Nano compared with Ti-Porous ($P = .042$), and it was not affected by implantation time point ($P = .947$; Figure 3f).

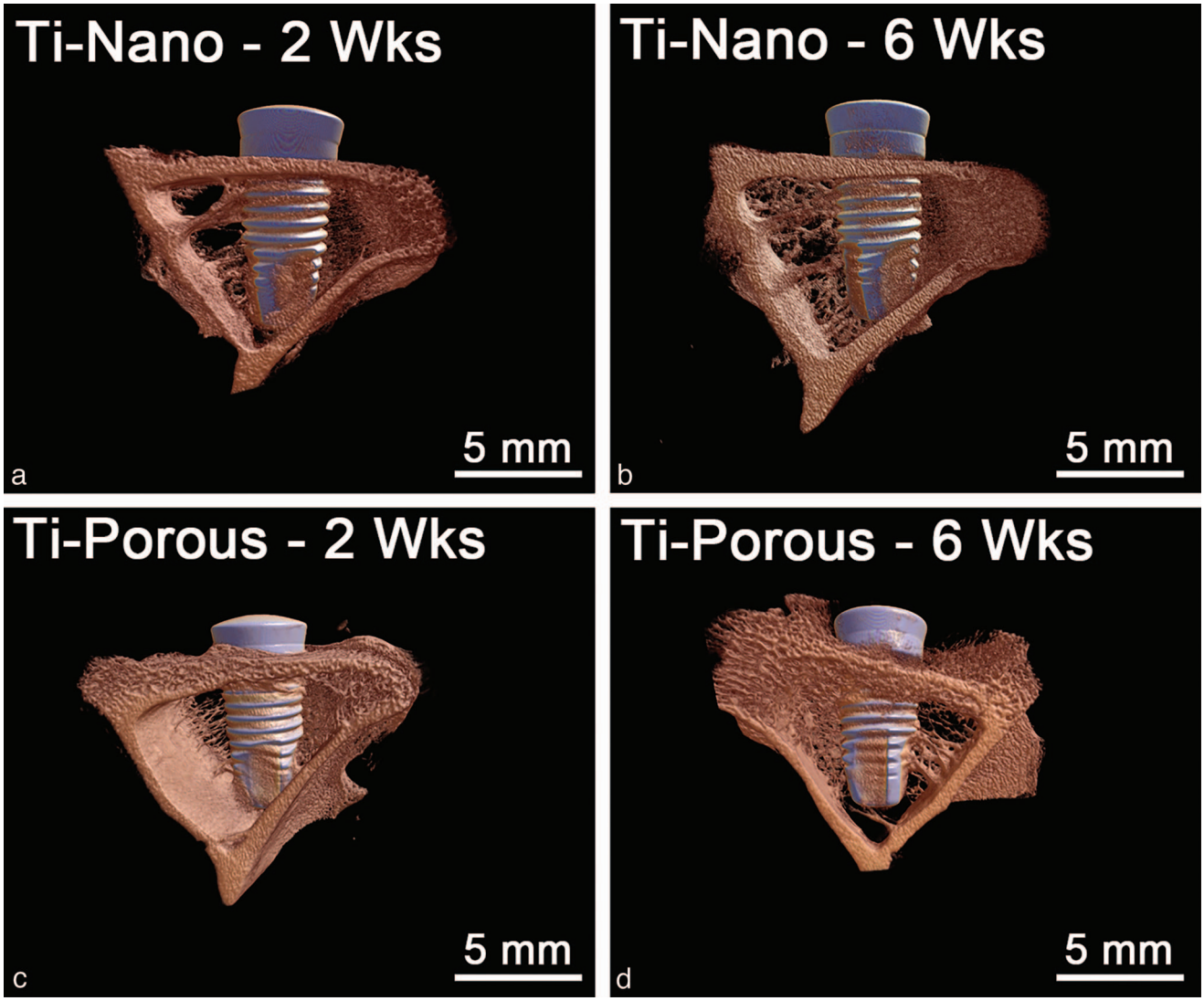

Figure 2. Three-dimensional reconstructed micro-CT images of rabbit tibia implanted with Ti-Nano (a, b) and Ti-Porous (c, d) at 2 weeks (a, c) and 6 weeks (b, d).

Histomorphometric analysis

At 2 weeks, Ti-Nano and Ti-Porous implants were surrounded by parent, lamellar trabecular bone with wide medullary areas (Figure 4a and c). Although no major histological changes in bone architecture were observed from 2 to 6 weeks, the trabecular bone exhibited reduced medullary areas at 6 weeks (Figure 4b and d). The percentage of BIC was not affected by surface topography of Ti implants ($P = .180$), and it decreased ($P = .021$) from 2 to 6 weeks (Figure 5a). The percentage of BABT was not affected either by surface topography of Ti implants ($P = .654$) or by implantation time point ($P = .201$; Figure 5b). The percentage of BAMA was not affected either by surface topography of Ti implants ($P = .250$) or by implantation time point ($P = .075$; Figure 5c).

Removal torque analysis

At 6 weeks, the removal torque was not affected by surface topography of Ti implants ($P = .093$; Figure 6).

Discussion

A wide range of surface modifications using different methods has been proposed to enhance and/or accelerate the process of osseointegration of Ti implants.[17,18] Such modifications are of particular interest in clinical situations involving type IV bone, which is primarily found in the posterior maxilla and has a lower success rate compared with other oral bone sites.[19] Here, we compared the bone response to a machined Ti implant treated with a mixture of H_2SO_4/H_2O_2 to generate nanotopography with a commercially available Ti implant with microtopography placed in rabbit tibia, a bone tissue similar to type IV bone.[20,21] The results showed bone formation in close contact with both Ti implant surfaces and no remarkable histological or morphometric differences, confirmed by the same torque needed to remove the implants irrespective of surface topography.

The surface treatment used in this study is an inexpensive and feasible approach to generate nanotopography on

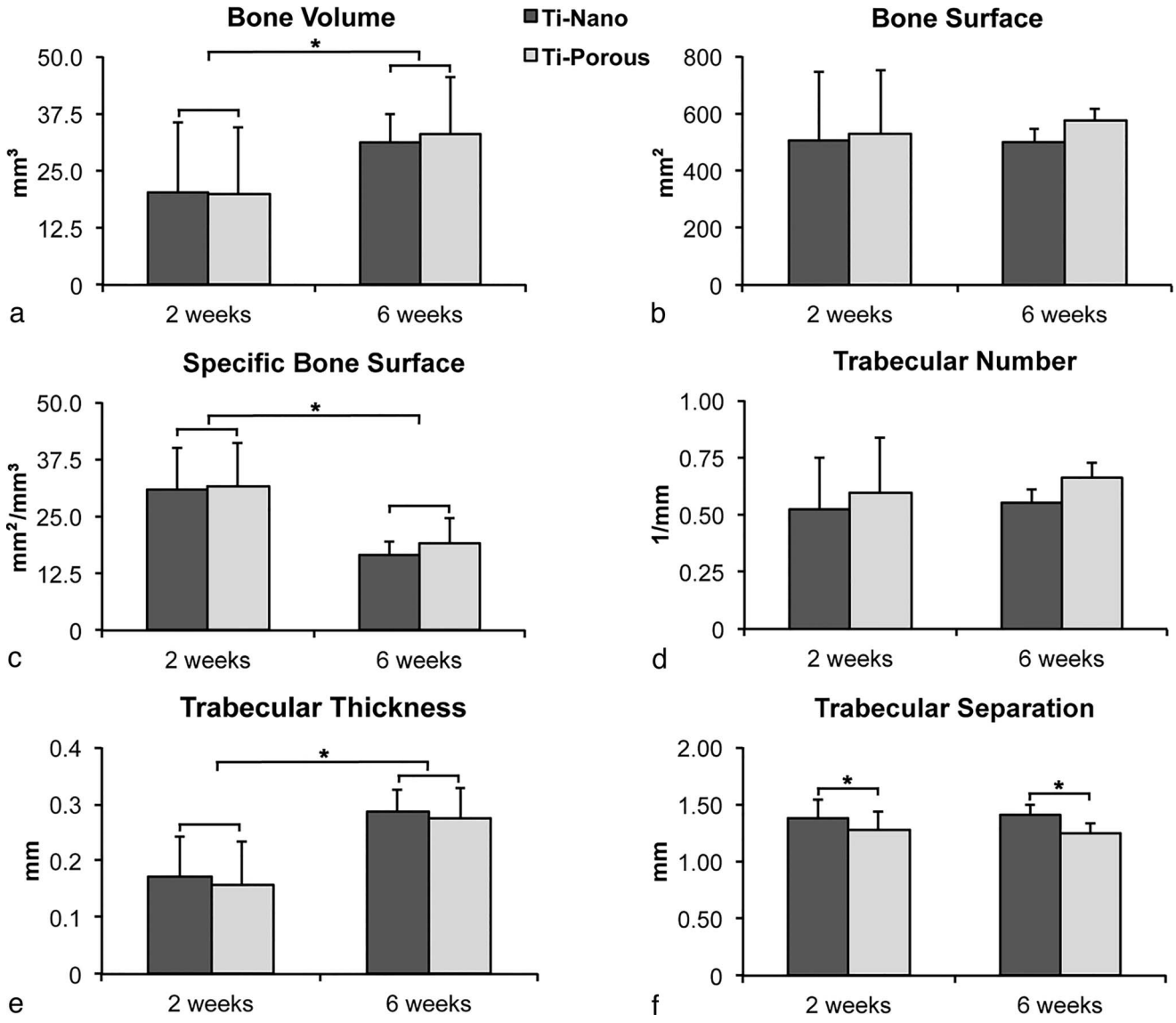

Figure 3. Morphometric parameters, bone volume (a), bone surface (b), specific bone surface (c), trabecular number (d), trabecular thickness (e), and trabecular separation (f) obtained from 3-dimensional reconstructed micro-CT images of rabbit tibia implanted with Ti-Nano and Ti-Porous at 2 and 6 weeks. Data are presented as mean ± standard deviation (n = 6). Asterisks indicate statistically significant difference ($P \leq .05$).

Ti implants.[13,14] This method is reproducible, as the topographical characteristics we observed are similar to those described elsewhere.[1,22] However, in a previous study by our group, it was noticed that this chemical treatment using the same parameters produced a Ti implant surface with microtopography instead of nanotopography.[7] As both studies were conducted with implants from different companies, such discrepancy may be attributed to the proprietary handling of the surface after machining, which could affect the process of deoxidation and reoxidation of Ti induced by H_2SO_4/H_2O_2.

The hard-tissue histology is a useful tool to bidimensionally evaluate histomorphometric parameters such as BIC, BABT, and BAMA and to describe morphological features of tissues; however, this methodology does not allow for the production of 3-dimensional reconstructions from serial sections.[23] To cover bi- and 3-dimensional features of bone tissue formed in contact with Ti implants, the morphometric analyses were performed on both undecalcified histological sections and 3-dimensional images obtained from micro-CT following previously established parameters.[24]

Among 9 histomorphometric parameters analyzed, only trabecular separation was statistically significant different between Ti-Nano and Ti-Porous implants, being higher on the latter, which is not biologically relevant and could not be attributed to surface topographies. In agreement with this, histological findings did not reveal meaningful differences in terms of bone formation that could be associated with any surface feature, in addition to a similar removal torque level of Ti-Nano and Ti-Porous implants. Moreover, the same pattern

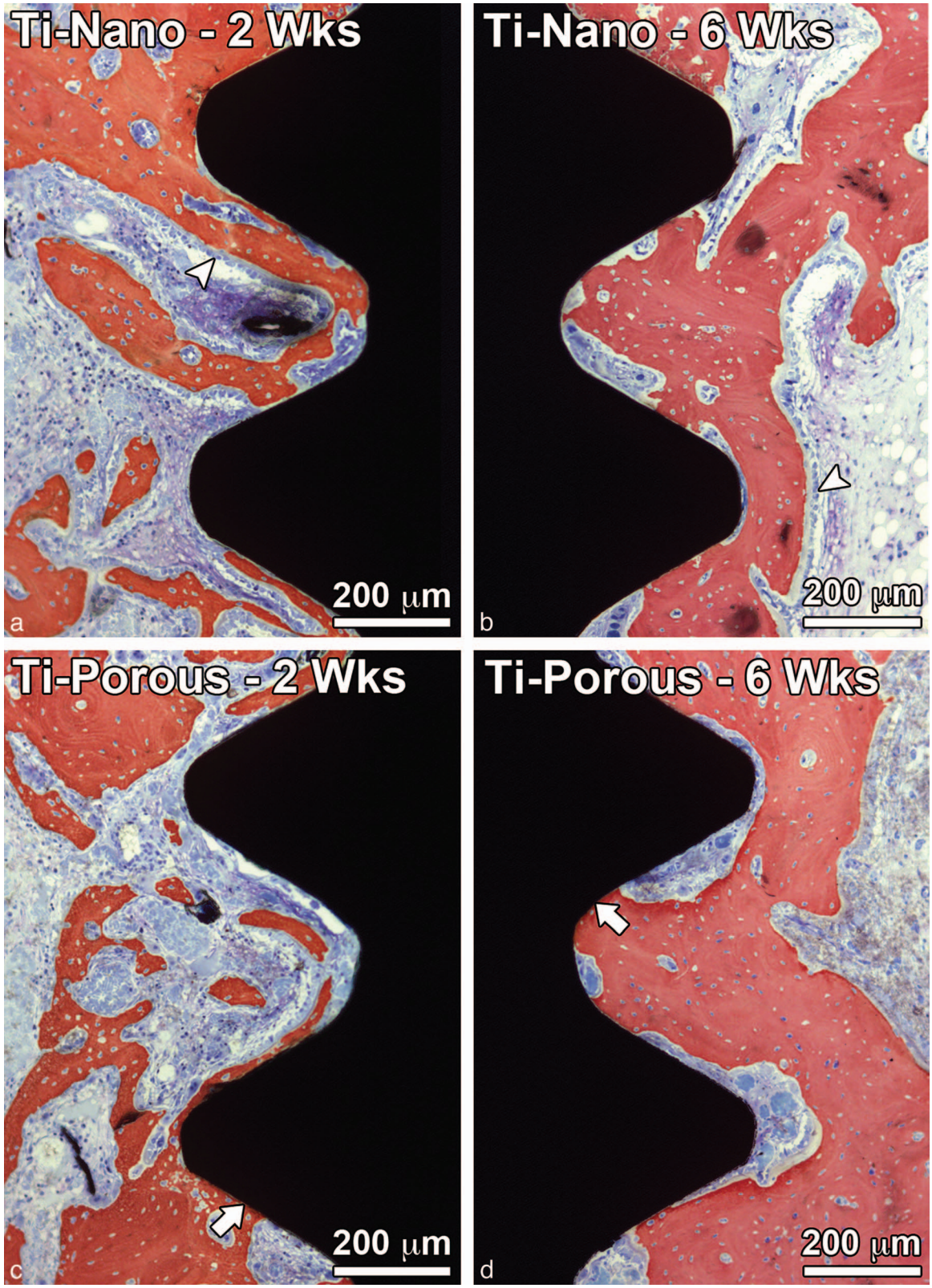

Figure 4. Mesiodistal ground sections of rabbit tibia implanted with Ti-Nano (a, b) and Ti-Porous (c, d) at 2 weeks (a, c) and 6 weeks (b, d). Arrowheads (a and b) indicate layers of active osteoblasts and arrows (c and d), bone-to-implant contact. Alizarin red and Stevenel's blue.

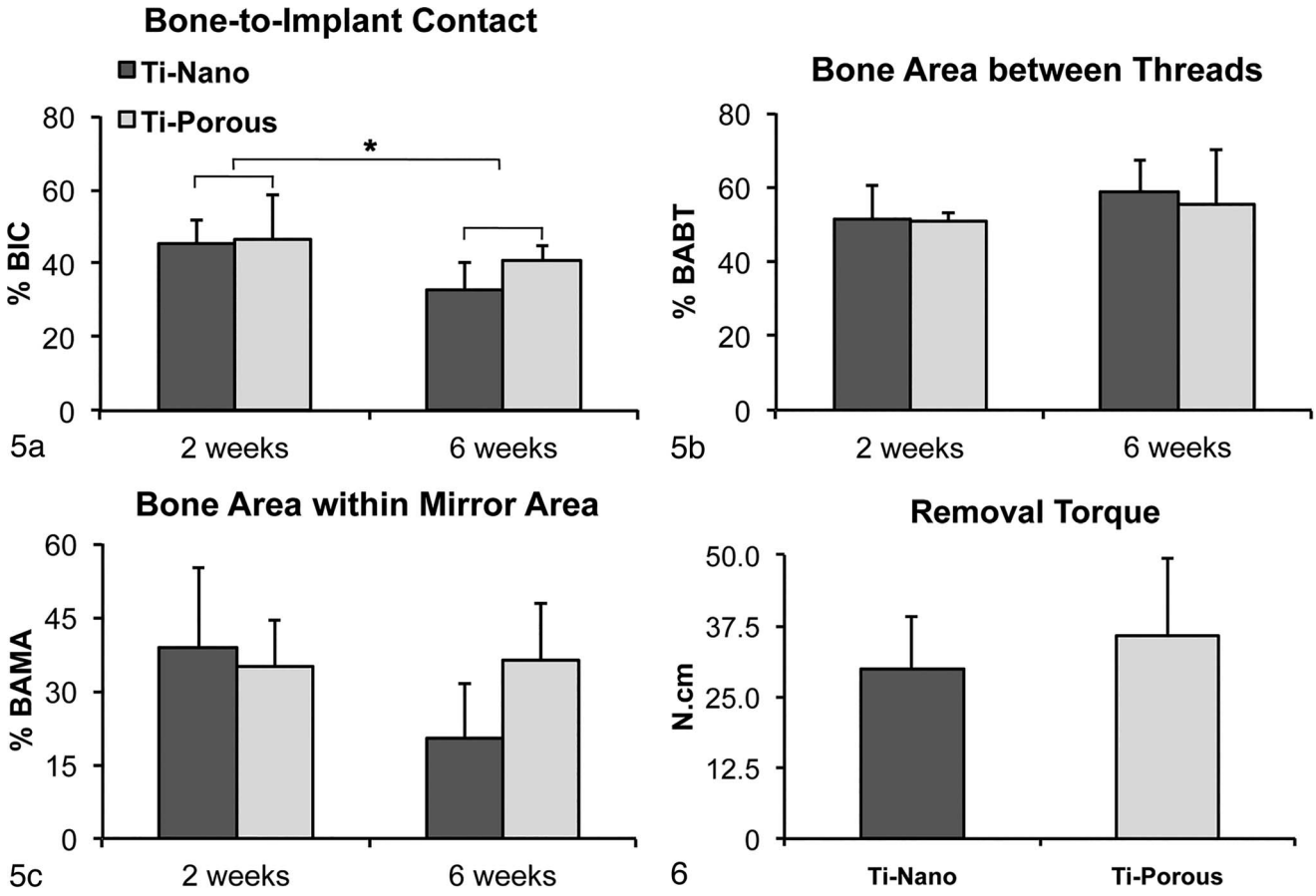

Figures 5–6. Figure 5. Morphometric parameters, bone-to-implant contact (BIC; a), mineralized bone area between threads (BABT; b), and mineralized bone area within mirror area (BAMA; c) obtained from mesiodistal ground sections of rabbit tibia implanted with Ti-Nano and Ti-Porous at 2 and 6 weeks. Data are presented as mean ± standard deviation (n = 6). Asterisks indicate statistically significant difference ($P \leq .05$). **Figure 6.** Removal torque of Ti-Nano and Ti-Porous at 6 weeks. Data are presented as mean ± standard deviation (n = 6).

of contact osteogenesis with bone growing on both surfaces was observed, suggesting the occurrence of bone bonding similar to that described for calcium phosphate-based materials,[25,26] which might also develop on metal surfaces.[27–29] However, the contact osteogenesis of Ti-Nano and Ti-Porous implants may not be the result of the same cellular mechanisms. Although we have shown that the interactions between osteoblastic cells and Ti-Nano involve an $\alpha 1\beta 1$ integrin signaling pathway and a miR-SMAD-BMP2 circuit,[10,11] the mechanism behind the response of osteoblasts to Ti-Porous remains to be determined.

Despite the absence of remarkable differences in bone formation on micro- and nanotopography surfaces, the implantation period influenced some of the histomorphometric parameters such as BIC and bone volume, which decreased and increased over time, respectively. Such effect of time indicates the dynamic process of bone remodeling around Ti implant surfaces from 2 to 6 weeks, with 6 weeks being a time point at which the process of bone formation is completed in this animal model.[30] Besides, the unexpected reduction of BIC from 2 to 6 weeks, mainly on Ti-Nano, could be due to the rise of locomotor load with time of healing. Indeed, this load may induce fails on the bone-metal interface of implants presenting nanotopography but not on surfaces with a combination of micro- and nanotopography.[27]

The benefits of surfaces presenting topographies at different scale levels supports the use of H_2SO_4/H_2O_2 combined with other techniques to generate hierarchical micro- and nanostructured surfaces. In addition, the association with bioactive molecules that promote osteoblast adhesion and activity could be a powerful complement to the nanotopography as the treatment with H_2SO_4/H_2O_2 facilitating surface functionalization.[8,31] In the context of clinical applications, the development of novel Ti surfaces based on functionalized micro-/nanotopography could represent an advance in implant therapy for patients with compromised bone tissue in terms of amount and architecture.

Conclusion

Our results have shown that the use of H_2SO_4/H_2O_2 is highly efficient in producing Ti surfaces with nanotopography, which elicits a similar bone response compared with a microtopography presented in a commercially available Ti implant. Thus, this simple and low-cost method to create nanotopography

could be a good alternative to generating Ti surfaces for long-term interfacial stability.

Abbreviations

BABT: bone area between threads
BAMA: bone area within mirror area
BIC: bone-to-implant contact
CT: computerized tomography
SEM: scanning electron microscopy

Acknowledgments

The authors would like to thank National Council for Scientific and Technological Development (CNPq) for financial support. Sebastiao C. Bianco is acknowledged for technical assistance during the experiments.

References

1. de Oliveira PT, Nanci A. Nanotexturing of titanium-based surfaces upregulates expression of bone sialoprotein and osteopontin by cultured osteogenic cells. *Biomaterials*. 2004;25:403–413.

2. Ban S, Iwaya Y, Kono H, Sato H. Surface modification of titanium by etching in concentrated sulfuric acid. *Dent Mater*. 2006;22:1115–1120.

3. Ahn S, Vang MS, Yang HS, Park SW, Lim HP. Histologic evaluation and removal torque analysis of nano- and microtreated titanium implants in the dogs. *J Adv Prosthodont*. 2009;1:75–84.

4. Jia F, Zhou L, Li S, et al. Phosphoric acid and sodium fluoride: a novel etching combination on titanium. *Biomed Mater*. 2014;9:035004.

5. Kieswetter K, Schwartz Z, Hummert TW, et al. Surface roughness modulates the local production of growth factors and cytokines by osteoblast-like MG-63 cells. *J Biomed Mater Res*. 1996;32:55–63.

6. Rosa AL, Beloti MM. Effect of cpTi surface roughness on human bone marrow cell attachment, proliferation, and differentiation. *Braz Dent J*. 2003;14:16–21.

7. Tavares MG, de Oliveira PT, Nanci A, Hawthorne AC, Rosa AL, Xavier SP. Treatment of a commercial, machined surface titanium implant with H2SO4/H2O2 enhances contact osteogenesis. *Clin Oral Implants Res*. 2007; 18:452–458.

8. Bueno RB, Adachi P, Castro-Raucci LM, Rosa AL, Nanci A, de Oliveira PT. Oxidative nanopatterning of titanium surfaces promotes production and extracellular accumulation of osteopontin. *Braz Dent J*. 2011;22:179–184.

9. Khang D, Choi J, Im YM, et al. Role of subnano-, nano- and submicron-surface features on osteoblast differentiation of bone marrow mesenchymal stem cells. *Biomaterials*. 2012;33:5997–6007.

10. Kato RB, Roy B, de Oliveira FS, et al. Nanotopography directs mesenchymal stem cells to osteoblast lineage through regulation of microRNA-SMAD-BMP-2 circuit. *J Cell Physiol*. 2014;229:1690–1696.

11. Rosa AL, Kato RB, Castro Raucci LM, et al. Nanotopography drives stem cell fate toward osteoblast differentiation through $\alpha 1\beta 1$ integrin signaling pathway. *J Cell Biochem*. 2014;115:540–548.

12. Shah FA, Nilson B, Brånemark R, Thomsen P, Palmquist A. The bone-implant interface-nanoscale analysis of clinically retrieved dental implants. *Nanomedicine*. 2014;10:1729–1737.

13. Yi J-H, Bernard C, Variola F, et al. Characterization of a bioactive nanotextured surface created by controlled chemical oxidation of titanium. *Surf Sci*. 2006;600:4613–4621.

14. Variola F, Yi J-H, Richert L, Wuest JD, Rosei F, Nanci A. Tailoring the surface properties of Ti6Al4V by controlled chemical oxidation. *Biomaterials*. 2008;29:1285–1298.

15. de Oliveira PT, Zalzal SF, Beloti MM, Rosa AL, Nanci A. Enhancement of in vitro osteogenesis on titanium by chemically produced nanotopography. *J Biomed Mater Res A*. 2007;80:554–564.

16. Sverzut AT, de Albuquerque GC, Crippa GE, et al. Bone tissue, cellular, and molecular responses to titanium implants treated by anodic spark deposition. *J Biomed Mater Res A*. 2012;100:3092–3098.

17. Dohan Ehrenfest DM, Coelho PG, Kang BS, Sul YT, Albrektsson T. Classification of osseointegrated implant surfaces: materials, chemistry and topography. *Trends Biotechnol*. 2010;28:198–206.

18. Wennerberg A, Albrektsson T. Current challenges in successful rehabilitation with oral implants. *J Oral Rehabil*. 2011;38:286–294.

19. Jaffin RA, Berman CL. The excessive loss of Branemark fixtures in type IV bone: a 5-year analysis. *J Periodontol*. 1991;62:2–4.

20. Sennerby L, Thomsen P, Ericson LE. A morphometric and biomechanic comparison of titanium implants inserted in rabbit cortical and cancellous bone. *Int J Oral Maxillofac Implants*. 1992;7:62–71.

21. Mapara M, Thomas BS, Bhat KM. Rabbit as an animal model for experimental research. *Dent Res J*. 2012;9:111–118.

22. Vetrone F, Variola F, de Oliveira PT, et al. Nanoscale oxidative patterning of metallic surfaces to modulate cell activity and fate. *Nano Lett*. 2009;9:659–665.

23. Stiller M, Rack A, Zabler S, et al. Quantification of bone tissue regeneration employing beta-tricalcium phosphate by three-dimensional non-invasive synchrotron micro-tomography: a comparative examination with histomorphometry. *Bone*. 2009;44:619–628.

24. Bouxsein ML, Boyd SK, Christiansen BA, Guldberg RE, Jepsen KJ, Müller R. Guidelines for assessment of bone microstructure in rodents using micro-computed tomography. *J Bone Miner Res*. 2012;25:1468–1486.

25. Takemoto M, Fujibayashi S, Neo M, Suzuki J, Kokubo T, Nakamura T. Bone-bonding ability of a hydroxyapatite coated zirconia-alumina nano-composite with a microporous surface. *J Biomed Mater Res A*. 2006;78:693–701.

26. Kawai T, Takemoto M, Fujibayashi S, et al. Comparison between alkali heat treatment and sprayed hydroxyapatite coating on thermally-sprayed rough Ti surface in rabbit model: effects on bone-bonding ability and osteoconductivity. *J Biomed Mater Res B Appl Biomater*. 2015;103:1069–1081.

27. Davies JE, Mendes VC, Ko JC, Ajami E. Topographic scale-range synergy at the functional bone/implant interface. *Biomaterials*. 2014;35:25–35.

28. Davies JE, Ajami E, Moineddin R, Mendes VC. The roles of different scale ranges of surface implant topography on the stability of the bone/implant interface. *Biomaterials*. 2013;34:3535–3546.

29. Davies JE. Bone bonding at natural and biomaterial surfaces. *Biomaterials*. 2007;28:5058–5067.

30. Ivanoff CJ, Sennerby L, Lekholm U. Influence of mono- and bicortical anchorage on the integration of titanium implants: a study in the rabbit tibia. *Int J Oral Maxillofac Surg*. 1996;25:229–235.

31. Variola F, Brunski JB, Orsini G, Tambasco de Oliveira P, Wazen R, Nanci A. Nanoscale surface modifications of medically relevant metals: state-of-the art and perspectives. *Nanoscale*. 2011;3:335–353.